GEOPHYSICS, VOL. 38, NO. 6 (DECEMBER 1973), P. 1130–1144, 13 FIGS.

RESISTIVITY, SELF-POTENTIAL, AND INDUCED-POLARIZATION SURVEYS OF A VAPOR-DOMINATED GEOTHERMAL SYSTEM†

A. A. R. ZOHDY*, L. A. ANDERSON*, AND L. J. P. MUFFLER‡

The Mud Volcano area in Yellowstone National Park provides an example of a vapor-dominated geothermal system. A test well drilled to a depth of about 347 ft penetrated the vapor-dominated reservoir at a depth of less than 300 ft. Subsequently, 16 vertical electrical soundings (VES) of the Schlumberger type were made along a 3.7-mile traverse to evaluate the electrical resistivity distribution within this geothermal field. Interpretation of the VES curves by computer modeling indicates that the vapor-dominated layer has a resistivity of about 75–130 ohm-m and that its lateral extent is about 1 mile. It is characteristically overlain by a low-resistivity layer of about 2–6.5 ohm-m, and it is laterally confined by a layer of about 30 ohm-m. This 30-ohm-m layer, which probably represents hot water circulating in low-porosity rocks, also underlies most of the survey area at an average depth of about 1000 ft.

Horizontal resistivity profiles, measured with two electrode spacings of an AMN array, qualitatively corroborate the sounding interpretation. The profiling data delineate the southeast boundary of the geothermal field as a distinct transition from low to high apparent resistivities. The northwest boundary is less distinctly defined because of the presence of thick lake deposits of low resistivities.

A broad positive self-potential anomaly is observed over the geothermal field, and it is interpretable in terms of the circulation of the thermal waters. Induced-polarization anomalies were obtained at the northwest boundary and near the southeast boundary of the vapor-dominated field. These anomalies probably are caused by relatively high concentrations of pyrite.

INTRODUCTION

Geophysical surveys of geothermal areas, particularly with electrical methods, have been made in several parts of the world. In Italy, Schlumberger electrical soundings were made in Larderello (Breusse and Mathiez, 1956) and in the two areas of Monte Labbro and San Filippo near Monte Amiata (Alfano, 1961). These surveys were made in order to map high-resistivity limestone bedrock under a low-resistivity and impermeable cover. Faults thus delineated in the limestone bedrock were interpreted to be zones where natural steam was most likely to be found. In New Zealand the boundaries of geothermal fields in the Taupo volcanic zone were outlined by the use of Wenner soundings, Wenner horizontal profiles, and bipole-dipole total field apparent resistivity mapping (Banwell and MacDonald, 1965; Hatherton et al, 1966; Risk et al, 1970). In Turkey (Duprat, 1970) and in Taiwan (Cheng, 1970), Schlumberger soundings were used to map geothermal areas. In the U.S., reconnaissance resistivity measurements were made in the Salton Trough, Imperial Valley, California, by Meidav (1970) and by McEuen (1970).

Geothermal systems, according to White et al (1971), are of two types: hot-water systems and (of less common occurrence) vapor-dominated systems. The Geysers, California, Larderello, Italy, and the Mud Volcano area, Yellowstone National Park, are examples of vapor-dominated systems. Geochemically, water samples from springs and drill holes in the v
dominated systems are charac
concentrations of sulfate anions
trations of chlorides (<20 ppm
the spring waters may be rich
bonate instead of sulfate. The
sulfate-rich spring waters are
cally low (2 to 3) because of the
phuric acid from oxidation of r
sodium bicarbonate waters dis
have neutral pH values. In c
water systems are characteri
centrations of chlorides, and t
subsurface temperatures of 18
duce hot springs that deposit s

In May 1968, hole Y-11 was
Geological Survey in the M
Yellowstone National Park.
pulled from depths of both 30
lent eruption of water occurr
eruption that consisted almos

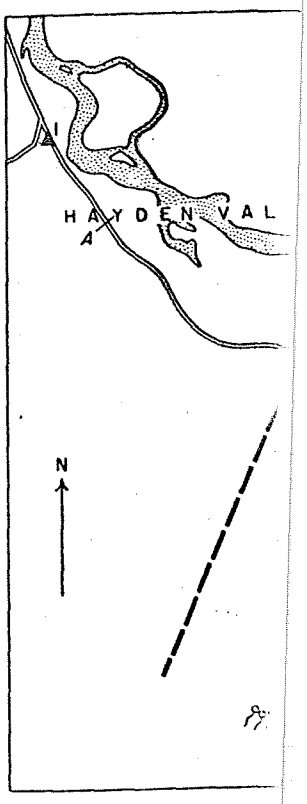

FIG. 1. Index map showing loc
thermal area. Resis

† Publication authorized by the Director, U.S. Geological Survey. Presented at the Symposium on Electrical Properties of Rocks, Salt Lake City, Utah, March 16, 1972. Manuscript received by the Editor June 6, 1973; revised manuscript received July 24, 1973.

* U.S. Geological Survey, Denver, Colo. 80225.

‡ U.S. Geological Survey, Menlo Park, Calif. 94025.

springs and drill holes in the vicinity of vapor-dominated systems are characterized by high concentrations of sulfate anions and low concentrations of chlorides (<20 ppm). Less commonly the spring waters may be rich in sodium bicarbonate instead of sulfate. The pH values of the sulfate-rich spring waters are also characteristically low (2 to 3) because of the formation of sulphuric acid from oxidation of rising H_2S gas. The sodium bicarbonate waters discharge feebly and have neutral pH values. In contrast, most hot-water systems are characterized by high concentrations of chlorides, and those systems with subsurface temperatures of 180°C or higher produce hot springs that deposit sinter.

In May 1968, hole Y-11 was drilled by the U.S. Geological Survey in the Mud Volcano area, Yellowstone National Park. After the core was pulled from depths of both 307 and 347 ft, a violent eruption of water occurred, followed by an eruption that consisted almost entirely of steam. White et al (1971) estimated that in these eruptions steam was associated with less than 10 percent liquid water by weight. For a hot water system to yield a comparable ratio of vapor to liquid, the permeability of the rocks must be low; but in Y-11, high rock permeabilities were evidenced by the large losses in circulation at all depths below 122 ft. Therefore, it must be the deficiency in liquid water, rather than the low permeability of rocks, that caused the steam to dominate the eruptions. Furthermore, according to White et al (1971), all the geochemical manifestations of vapor-dominated systems are exhibited in the Mud Volcano area.

Subsequent to the drilling of Y-11, the USGS made VES (vertical electrical sounding), resistivity horizontal profiles, SP (self-potential), and IP (induced-polarization) measurements in the Mud Volcano area to evaluate the geoelectrical properties of a section containing a vapor-dominated geothermal system.

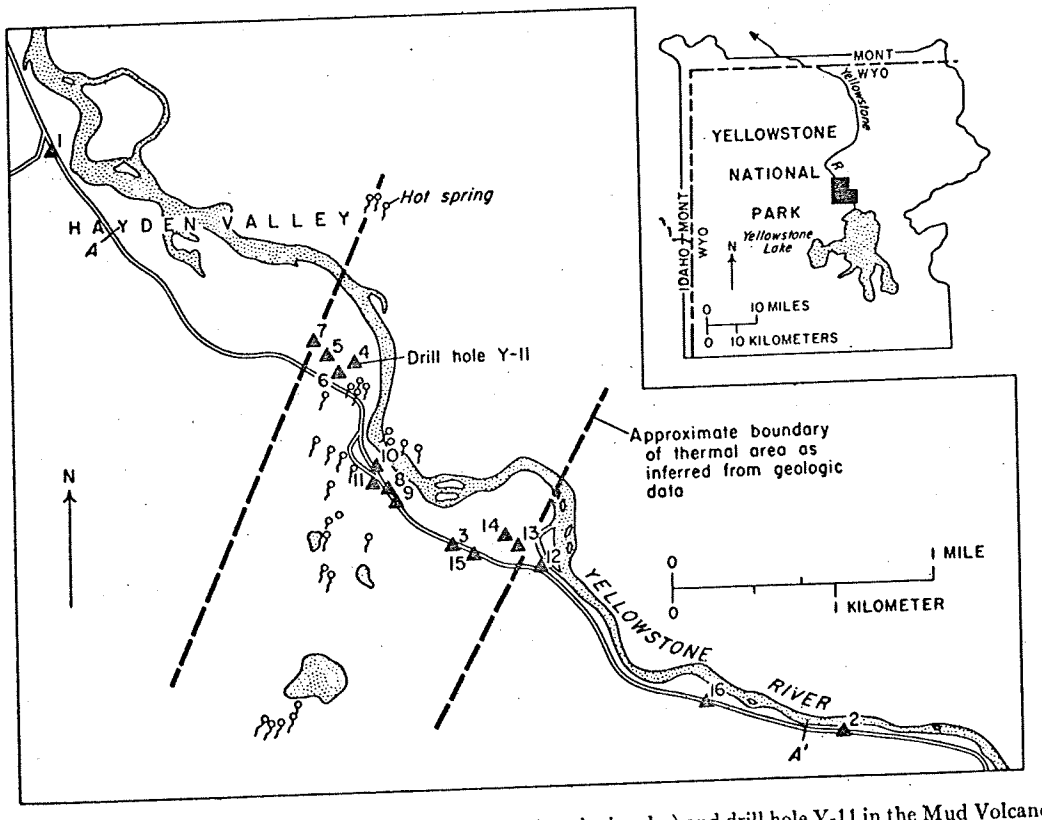

FIG. 1. Index map showing locations of VES stations (numbered triangles) and drill hole Y-11 in the Mud Volcano thermal area. Resistivity, SP, and IP profiles were measured along the road from A to A'.

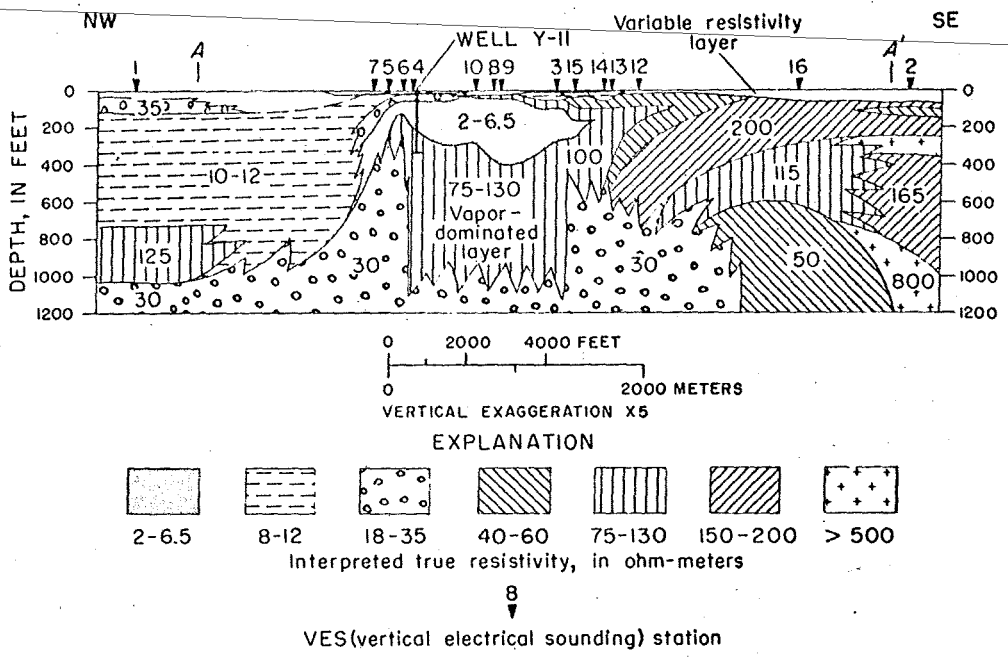

FIG. 2. Geoelectric section of the Mud Volcano area, Yellowstone National Park.

GENERAL SETTING

The Mud Volcano area (Figure 1) lies along the Yellowstone River approximately 5 miles north of Yellowstone Lake. Most of the area is covered by glacial silt, sand, and gravel which are underlain by rhyolitic ash-flow tuff; the area contains numerous mud pots and acid-sulfate springs. Some nearly neutral bicarbonate-sulfate springs occur along the river, but there are no chloride-rich springs in the area.

The location of the 16 VES stations, the test well Y-11, and the resistivity, SP, and IP profiles (which were made along the road from A to A') are shown in Figure 1. The approximate boundaries of the geothermal field, as inferred from geologic data are also shown.

THE GEOELECTRIC SECTION

Figure 2 shows the geoelectric section obtained from the interpretation of the VES curves. In the middle of the section, beneath VES 7 to VES 12, there are basically four electrical units. The first unit is composed of several near-surface layers, some of which are of small lateral extent (about 1,000 ft or less) and of variable resistivities. The second electrical unit is a fairly uniform single layer of remarkably low resistivity of about 2–6.5 ohm-m. It occurs at an average depth of about 50 ft and extends to an average depth of about 250 ft. This low-resistivity layer is interpreted as a layer where steam condenses into hot water, and where pyrite and clay minerals (kaolinite and montmorillonite) are present. The third electrical unit is a high-resistivity layer of about 75–130 ohm-m. Where this layer underlies the 2–6.5-ohm-m layer, it is interpreted as a zone where "dry steam," rather than liquid water, dominates the larger pores and open fractures in the rocks. The maximum depth to the bottom of this layer is unknown, but the minimum depth is about 1000 ft, and its lateral extent is approximately 1 mile. On both the northwest and southeast boundaries of this layer is the fourth geoelectric unit, a layer which is characterized by a resistivity of about 30 ohm-m and which is interpreted as a layer of hot water in low-porosity rocks.

At the northwest end of the section, beneath VES 1, there is a thick (about 600 ft) low-resistivity (10–12 ohm-m) layer which represents lacustrine deposits in Hayden Valley. In the southeastern part of the section, however, beneath VES 16 and VES 2, the layer resistivities generally are high (40–800 ohm-m) to depths of at least about 600 ft, thus reducing the probabil-

ity for the presence of therm
comparable to those at the n

INTERPRETATION OF

The 16 vertical electrical s
using the Schlumberger ar
electrode spacings (AB/2) r
3000 ft. Interpretation of t
made by curve-matching pro
bums of theoretical curves (C
1966; Rijkwaterstaat, 1969),
grams (Zohdy, 1965), Dar Z
method for the automatic i
curves (Zohdy, 1972) were
geologically and geoelectric
tion as well as to achieve
observed and calculated VE

The curve of VES 1 is sho
where it is matched with t
one calculated for a six-la
based on auxiliary point i
other calculated for a 19-
obtained by the computer
terpretation program. Th
cate the presence of eith

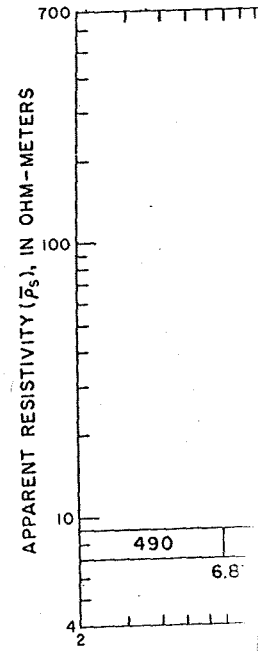

FIG. 3. Six-layer inter
subsequently verified by
preted true resistivities i

ity for the presence of thermal activity at depths comparable to those at the middle of the section.

INTERPRETATION OF VES CURVES

The 16 vertical electrical soundings were made using the Schlumberger array with maximum electrode spacings (AB/2) ranging from 500 to 3000 ft. Interpretation of the VES curves was made by curve-matching procedures in which albums of theoretical curves (Orellana and Mooney, 1966; Rijkwaterstaat, 1969), auxiliary point diagrams (Zohdy, 1965), Dar Zarrouk curves, and a method for the automatic interpretation of VES curves (Zohdy, 1972) were all used to reach a geologically and geoelectrically acceptable solution as well as to achieve excellent fits between observed and calculated VES curves.

The curve of VES 1 is shown in Figures 3 and 4, where it is matched with two theoretical curves, one calculated for a six-layer model (Figure 3), based on auxiliary point interpretation, and the other calculated for a 19-layer model that was obtained by the computer using the automatic interpretation program. The interpretations indicate the presence of either a sequence of low-resistivity layers (5–23 ohm-m) that extends from a depth of about 100 ft to a depth of about 1000 ft, or a single low-resistivity layer (11–12 ohm-m) that extends from a depth of about 100 ft to a depth of about 700 ft. This low-resistivity layer is probably composed of clayey and silty lake deposits and is not necessarily related to the geothermal system. It is underlain by one layer of 125 ohm-m or by two layers of 50 and 125 ohm-m, respectively. These layers are underlain by a thick layer of low resistivity ($\leq$35 ohm-m). Because of the lack of geologic information and other VES data in the immediate vicinity of this sounding, it is difficult to decide which interpretation is more accurate. The two interpretations are presented here to illustrate the problems of equivalence between multilayer sections in the interpretation of a single VES curve.

Figure 5 shows the curve of VES 7 and its interpretation in terms of a five-layer section. The third, fourth, and fifth layers are not clearly manifested on the VES curve, but correlation with the curves of VES 5 and VES 6, which are shown in Figure 6, clearly indicates that the small maximum and minimum on the curve of VES 7 (be-

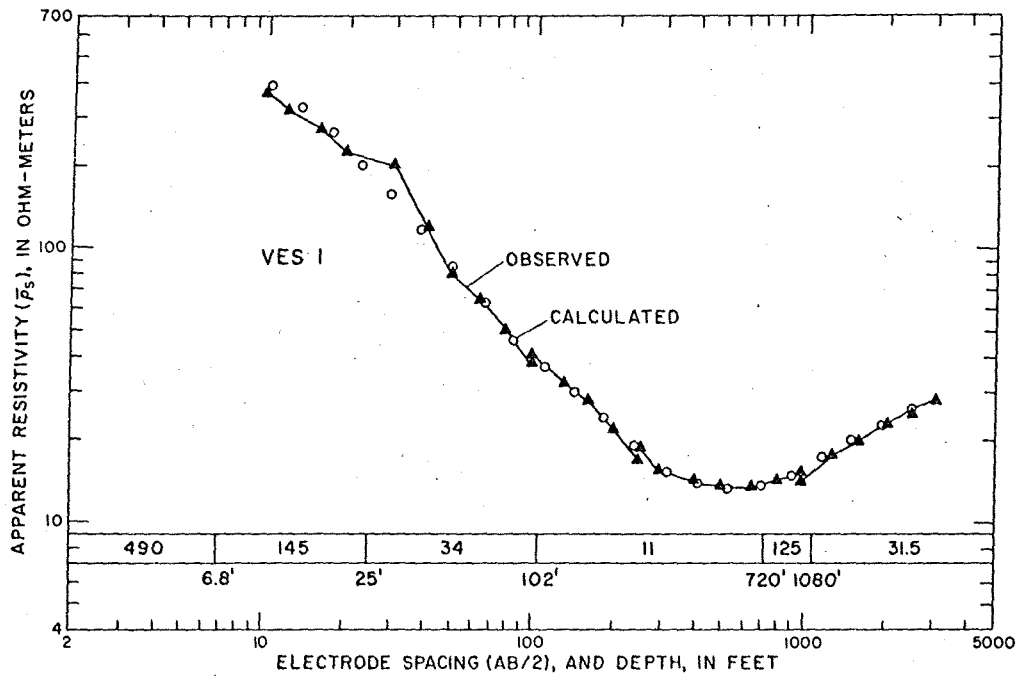

FIG. 3. Six-layer interpretation of VES 1 curve. Interpretation initially made with auxiliary point method and subsequently verified by computer calculation of interpreted model. Numbers in and below bar designate interpreted true resistivities in ohm-meters and interpreted depths in feet, respectively.

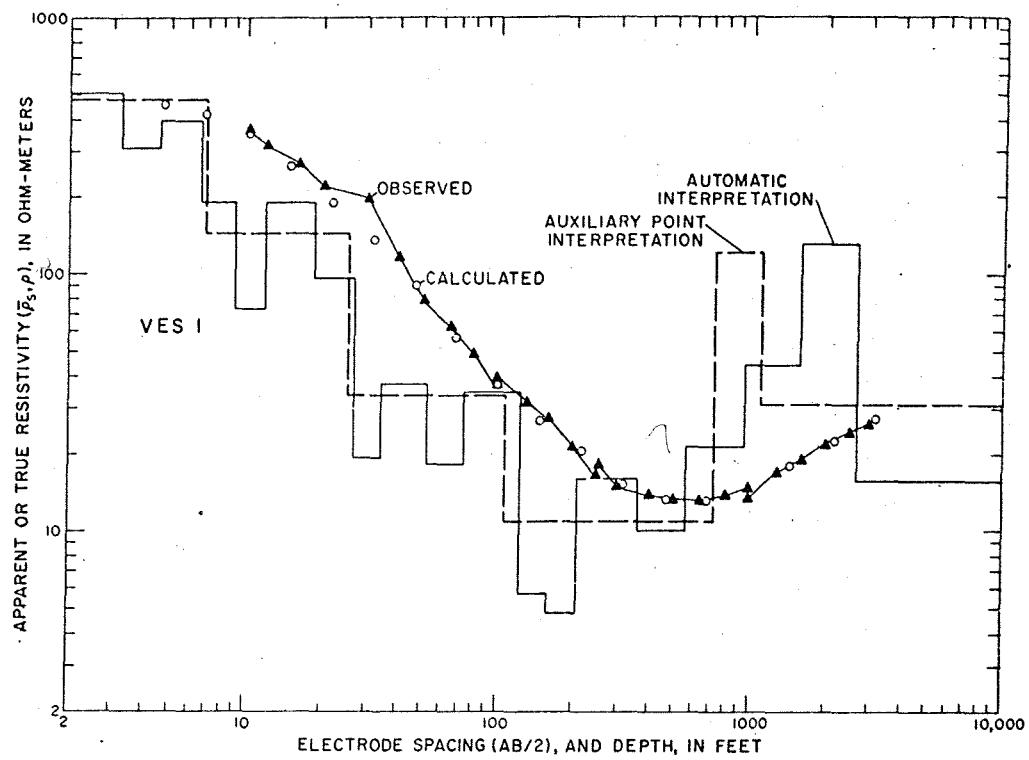

FIG. 4. Equivalence between 19-layer automatic interpretation and six-layer auxiliary point interpretation of VES 1 curve.

tween $AB/2 = 100$ and 1000 ft) are meaningful. They express the presence of the same layers that are represented by the well-developed maxima and minima on the curves of VES 5 and VES 6. The value of the apparent resistivity on the minimum of VES 6 is about 6.2 ohm-m and this is the first concrete evidence obtained on the northwest side of the section of the presence of a layer that must have a true resistivity of less than 6 ohm-m. For VES 6 the true resistivity of that layer is interpreted to be about 2 ohm-m, whereas for VES 5 and VES 7 it is interpreted to be about 4 and 4.5 ohm-m, respectively. The rising terminal branch on VES 7 curve is not well developed, but on the VES 5 curve the well-developed terminal branch indicates that the bottommost layer must have a resistivity of about 30 ohm-m. The curvature of the terminal branch of VES 6 curve is fitted best with a theoretical curve for a section in which a layer of about 75 ohm-m (or more) must exist between the very low (2 ohm-m) resistivity layer and the bottommost layer of about 30 ohm-m. This 75-ohm-m layer is interpreted to represent the northwest edge of the vapor-dominated layer.

The center of VES 4 was located about 100 ft north of well Y-11. The observed curve and its interpretation are shown in Figure 7 together with the geologic log of Y-11. The curve was interpreted in terms of a five-layer geoelectric section, the first layer of which has a resistivity of about 1700 ohm-m and a thickness of about 7 ft. The first layer corresponds to the layer of dry river gravel which lies within 6 inches above the water table. The second and third layers have resistivities of about 170 and 28 ohm-m, respectively, and extend to a depth of about 60 ft. These two layers correlate well with a layer of conglomerate composed of white pumice and black obsidian underlain by a layer of sandstone of the same composition. The depth to the bottom of the sandstone layer is about 65 ft which is in good agreement with the interpreted depth of about 60 ft. The fourth layer, on the interpreted geoelectric section beneath VES 4, has a low resistivity of

about 6.3 ohm-m and extend
195 ft where it is underlain
layer of about 120 ohm-m o
corresponding geologic form
the well is composed of ri
and it extends to the bottom
Mineralogical analysis of co
Y-11 (unpublished data o
L. J. P. Muffler) indicates t
pyrite are present from a
to the bottom of the well
posits occur at a depth of
tinue to exist to the bottom
at which these chalcedony
cellent agreement with the
195 ft to the high-resistivi

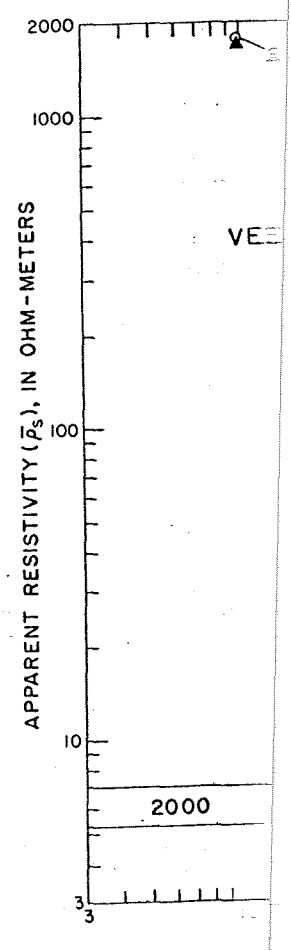

FIG. 5. Interpretation o
interpreted tru

about 6.3 ohm-m and extends to a depth of about 195 ft where it is underlain by a high-resistivity layer of about 120 ohm-m of large thickness. The corresponding geologic formation encountered in the well is composed of rhyolitic ash-flow tuff, and it extends to the bottom of the well at 347 ft. Mineralogical analysis of core samples from well Y-11 (unpublished data of K. E. Bargar and L. J. P. Muffler) indicates that clay minerals and pyrite are present from a depth of about 50 ft to the bottom of the well. Some chalcedony deposits occur at a depth of about 200 ft and continue to exist to the bottom of the well. The depth at which these chalcedony deposits occur is in excellent agreement with the interpreted depth of 195 ft to the high-resistivity layer of 120 ohm-m. Therefore, it is tempting to conclude that it is the chalcedony deposits that have caused the rise in resistivity. However, because the porosity of the ash-flow tuff (according to drilling data) did not change significantly at the depth of 200 ft, and because the conductive clay minerals and pyrite continue to exist in essentially the same amounts to the bottom of the well, we interpret the decrease in resistivity to about 6.3 ohm-m and its subsequent increase to about 120 ohm-m (on the curve of VES 4, as well as on the curves of VES 8, VES 9, and VES 10) to be governed mostly by the abundance of hot liquid water in the 2–6.5-ohm-m layer and by the dominance of steam in the 75–130-ohm-m layer. The drilling results of well Y-11 indicate that steam dominates

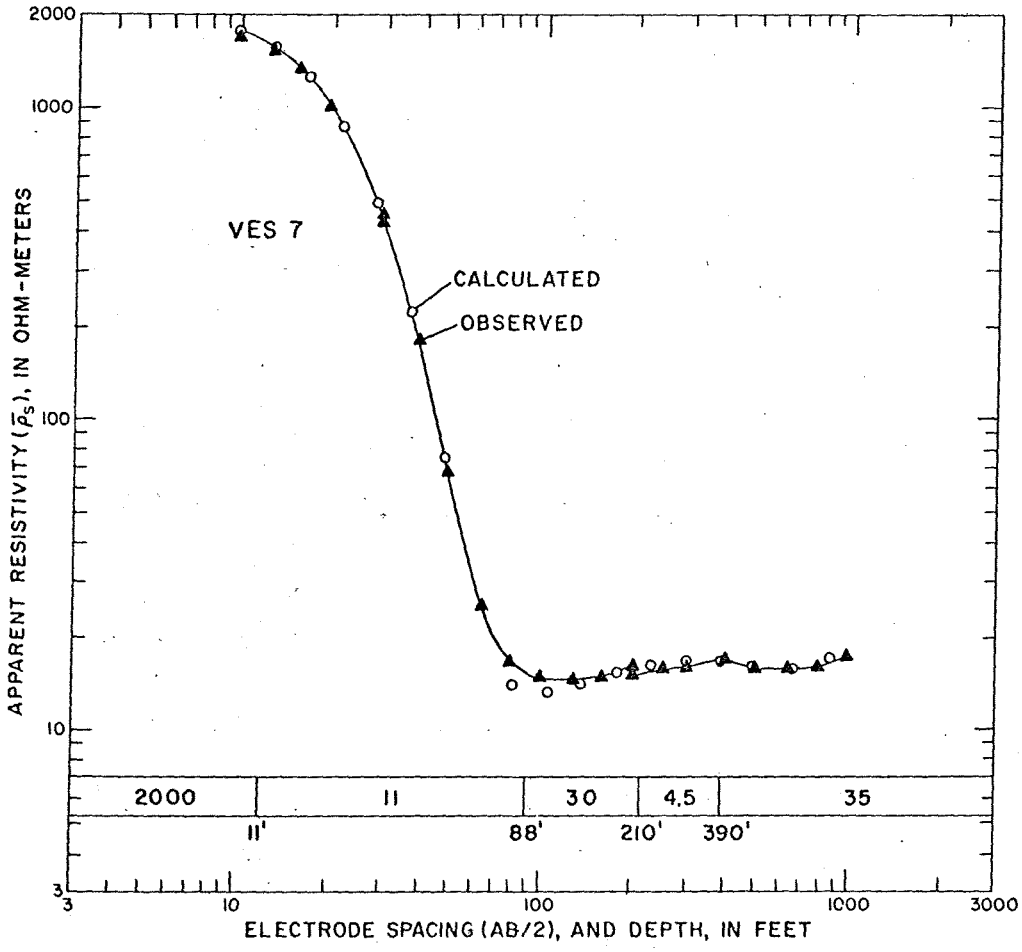

FIG. 5. Interpretation of VES 7 curve in terms of a five-layer model. Numbers in and below bar designate interpreted true resistivities, in ohm-meters, and interpreted depths, in feet, respectively.

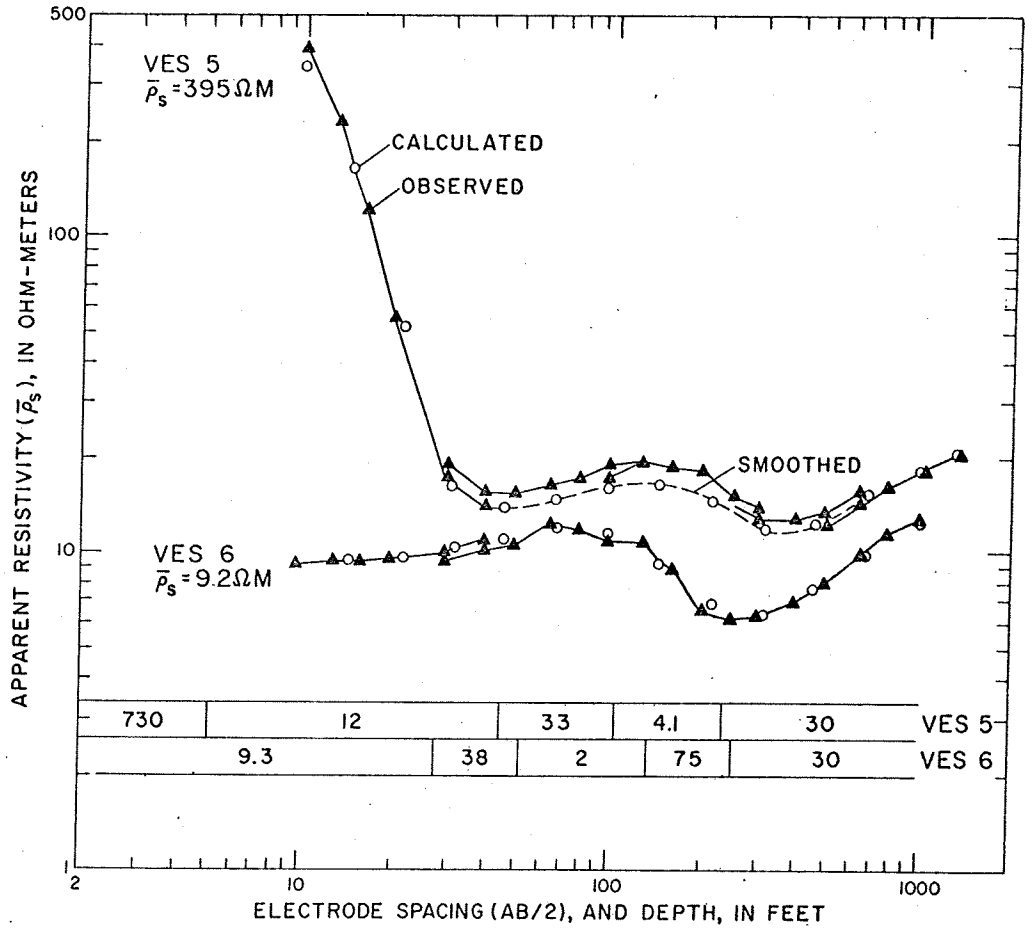

FIG. 6. Interpretation of VES 5 and VES 6 curves. Numbers in bars designate interpreted true resistivities, in ohm-meters.

the system from a depth of at least 307 ft to the bottom of the hole (White et al, 1971), but according to the interpretation of VES 4 the steam may dominate the system to a depth as shallow as 200 ft.

Figure 8 shows the curve of VES 10 which was obtained near the middle of the geothermal field (see Figure 2). The magnitude and the direction of the discontinuities on the observed curve (which were observed upon the expansion of the potential electrodes) are not in agreement with those prescribed for horizontal layering (Deppermann, 1954; Zohdy, 1969). Following a procedure which has been found to be most satisfactory in practice, the various segments on the VES curve were shifted to conform to the position of the last segment on the curve. The shifted segments then are smoothed, to remove cusps which are caused by the crossing of lateral heterogeneities by the current electrodes, and the smoothed curve is fitted with a theoretical one as shown in Figure 8 for VES 10. Similar smoothing was made for VES 5 and for other curves. This smoothing procedure results in modifying the interpreted true resistivities of the shallower layers in the section, which in general are quite variable, but it does not alter their interpreted thicknesses nor does it create undulations on the smoothed curve (which may be interpreted as layers) that were not actually manifested on the observed curve. These undulations often are created when the smoothing is made by drawing a curve that passes between

significantly displaced segme
interpreted depth to the var
beneath the low-resistivity la

The curves of VES 8, VES
their interpretations are sho
lustrate the continuity of t
conductive (2.4–5.2 ohm-m
(90–100 ohm-m) bottom la
curves. The interpreted dep
and about 400 ft, beneath
respectively, are the largest i
the resistive bottom layer ov
the geothermal section.

Figure 10 shows the curves
and VES 13 and their interp

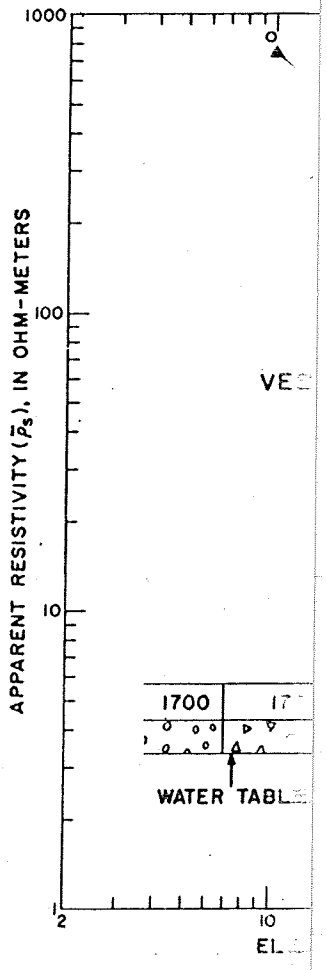

FIG. 7. Comparison between
designate interpreted true resist
posed of white pumice and black

significantly displaced segments. For VES 10 the interpreted depth to the vapor-dominated layer, beneath the low-resistivity layer, is about 300 ft.

The curves of VES 8, VES 9, and VES 3 and their interpretations are shown in Figure 9 to illustrate the continuity of the detection of the conductive (2.4–5.2 ohm-m) and the resistive (90–100 ohm-m) bottom layers on the VES curves. The interpreted depths of about 340 ft and about 400 ft, beneath VES 9 and VES 8, respectively, are the largest interpreted depths to the resistive bottom layer over the middle part of the geothermal section.

Figure 10 shows the curves of VES 15, VES 14, and VES 13 and their interpretations. Using the automatic interpretation computer program, the curve of VES 15 is the only curve in this group of VES curves that can be interpreted so that a layer with a low resistivity of about 5 ohm-m can be included legitimately in the section. Thus VES 15 reflects the nearness of the southeastern boundary of the geothermal system. On all three VES curves there is a strong indication that the bottommost layer, which lies at an average depth of about 550 ft, has a resistivity of about 30 ohm-m. This layer bounds the geothermal system on the southeast as it did on the northwest.

The curves of VES 12, VES 16, and VES 2 are shown in Figure 11 together with their interpretation as obtained for the reduced model of the

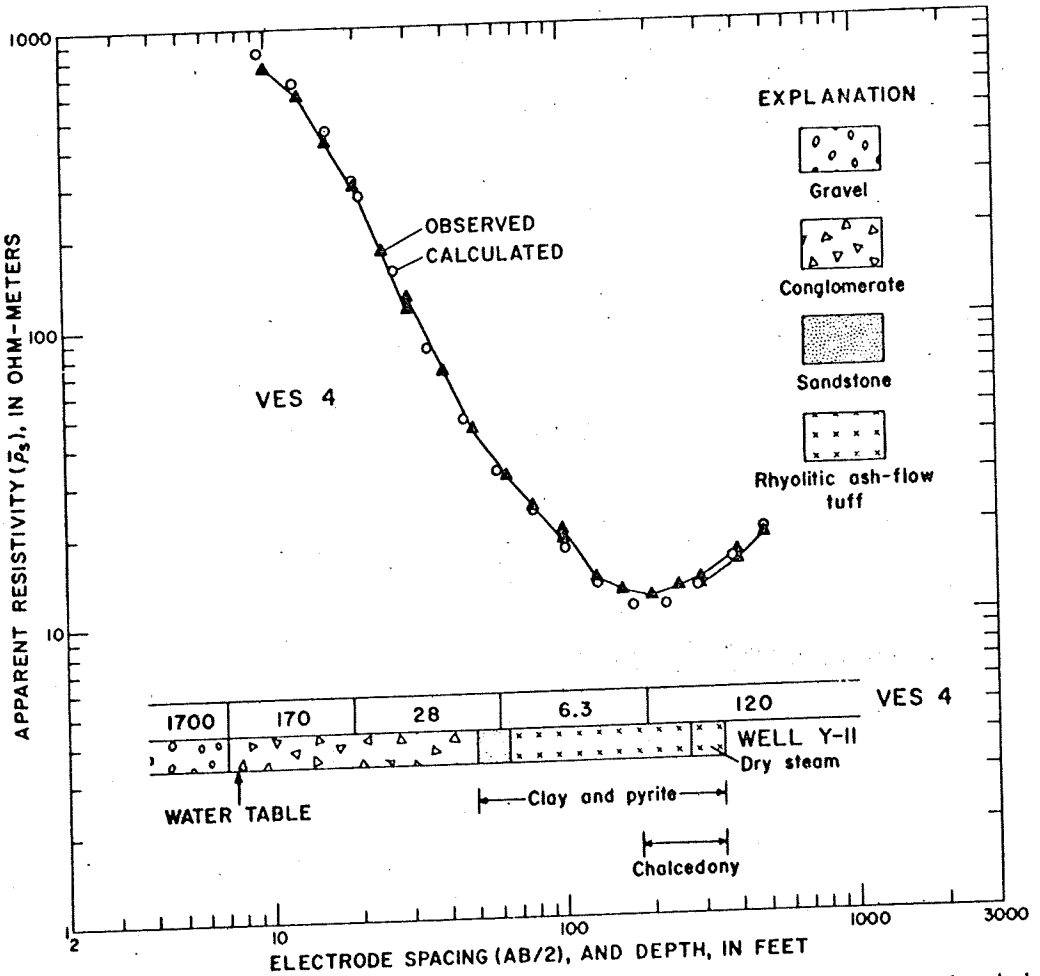

FIG. 7. Comparison between interpretation of VES 4 curve and geologic data of well Y-11. Numbers in bar designate interpreted true resistivities, in ohm-meters. Conglomerate and sandstone layers in well Y-11 are composed of white pumice and black obsidian.

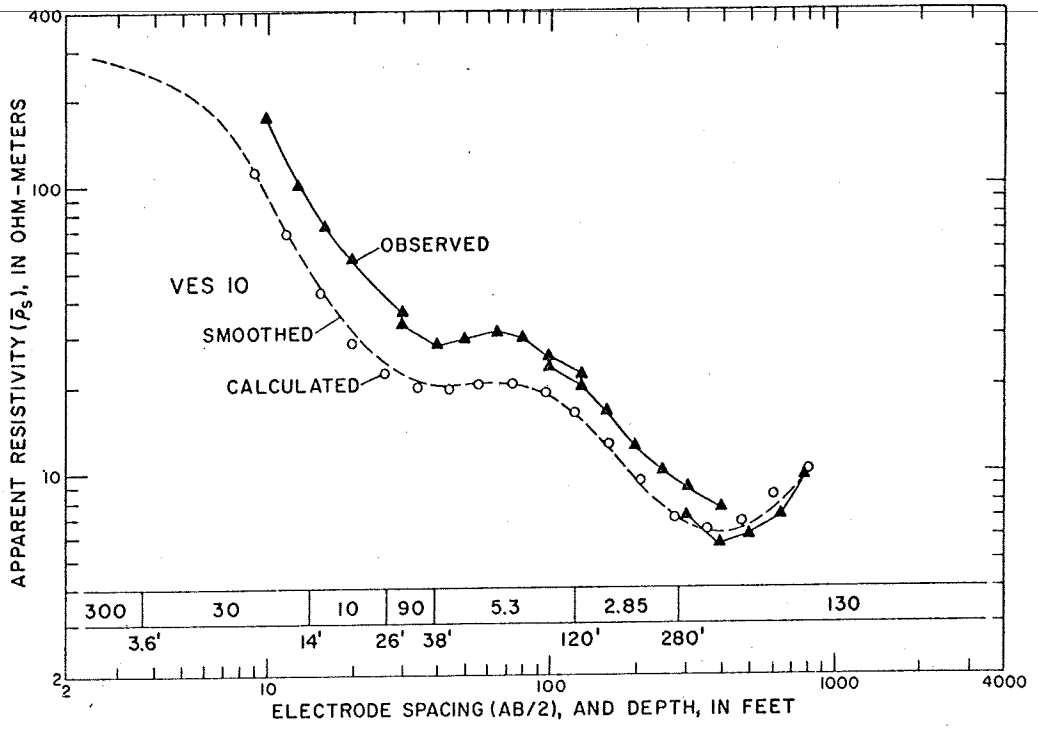

FIG. 8. Interpretation of VES 10 curve in terms of a seven-layer section. Numbers in and below bar designate interpreted true resistivities, in ohm-meters, and interpreted depths, in feet, respectively.

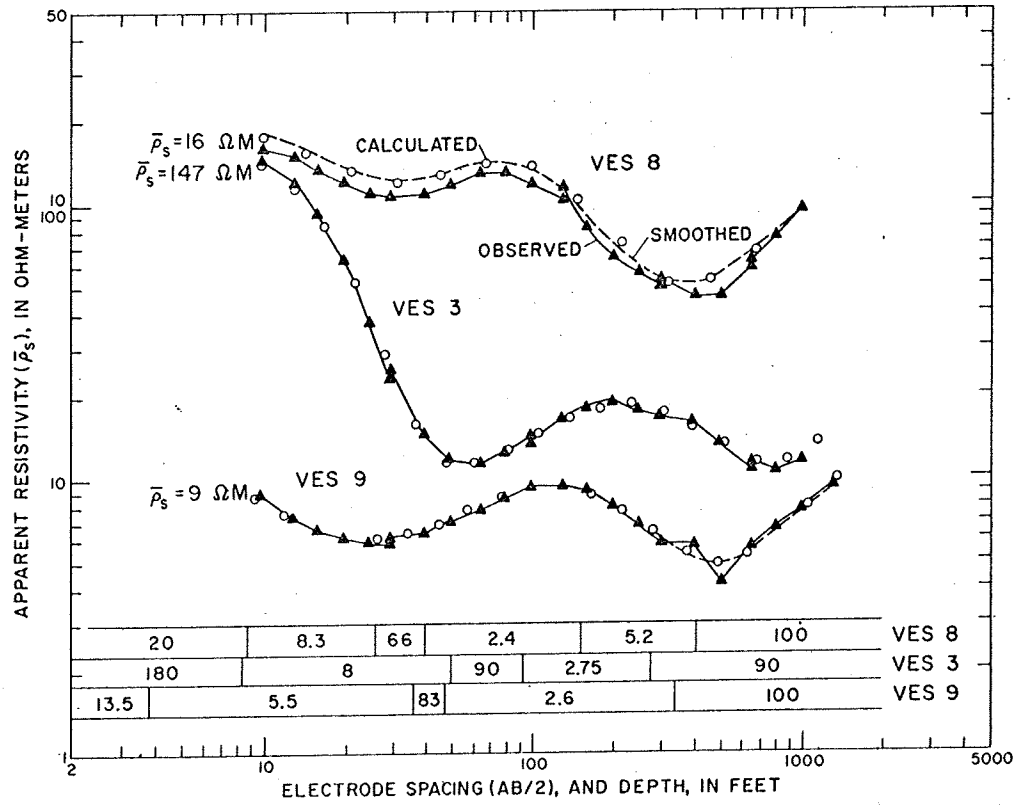

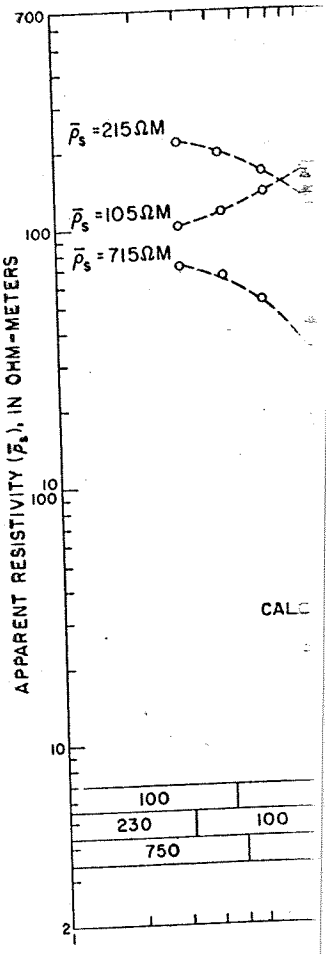

FIG. 10. Curves of VES 13
thermal field. Num

automatic interpretation cor
30-ohm-m bottom layer is
VES 2 curve, and if it exists
greater than about 1500
resistivity layers of 800 and
bottom layers in the auto
section, which indicates tha
thermal activity beneath
rhyolitic ash flow tuff belie

FIG. 9. Curves of V
Numbers

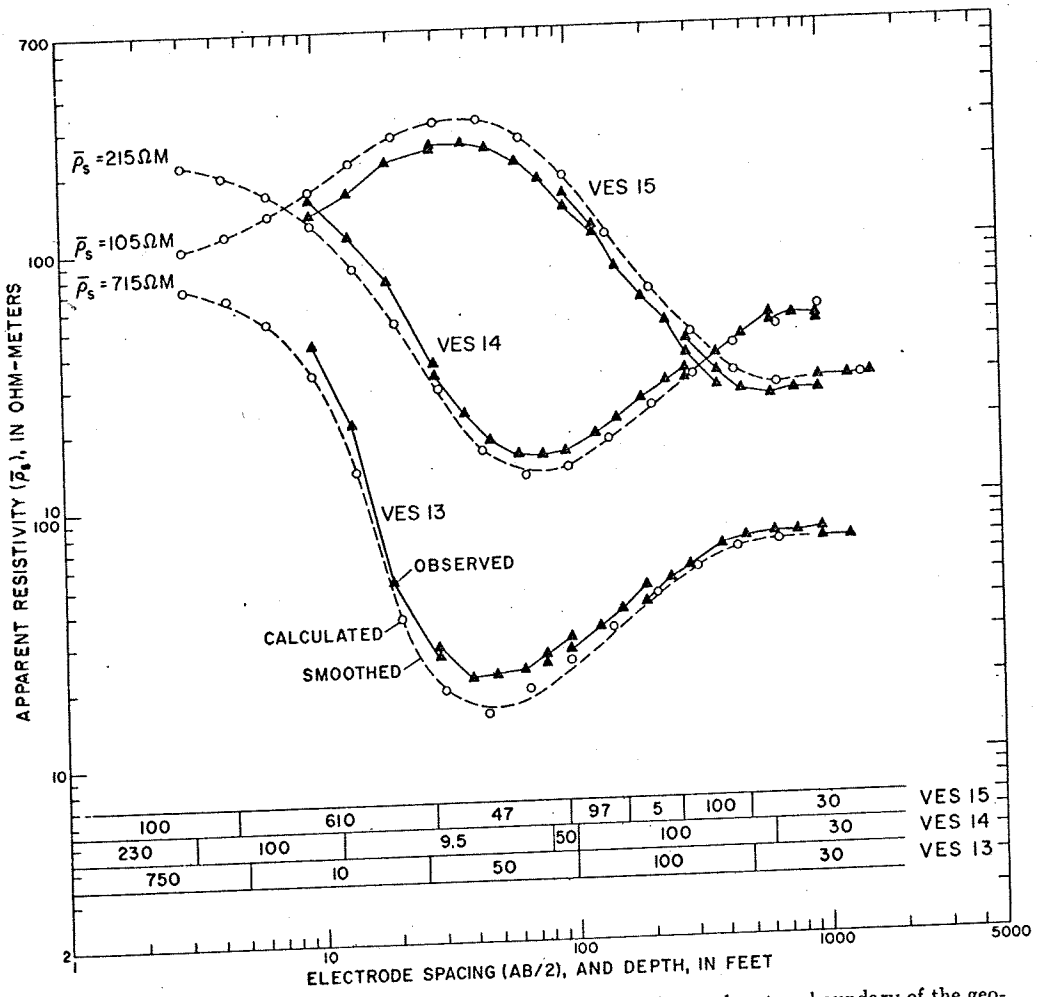

FIG. 10. Curves of VES 13, VES 14, and VES 15 obtained near the southeastern boundary of the geothermal field. Numbers in bars designate interpreted true resistivities, in ohm-meters.

automatic interpretation computer program. The 30-ohm-m bottom layer is not detected on the VES 2 curve, and if it exists it must be at a depth greater than about 1500 ft. Instead, high-resistivity layers of 800 and 300 ohm-m form the bottom layers in the automatically interpreted section, which indicates that there is no shallow thermal activity beneath VES 2 and that the rhyolitic ash flow tuff believed to form the bedrock in the area is probably replaced by rhyolite rocks of intermediate to high resistivities.

From the preceding description and documentation of the VES curves, and from the hydrogeologic information obtained from well Y-11, we conclude that the shallow vapor-dominated reservoir in the Mud Volcano area has a high resistivity of about 75–130 ohm-m and that it is characterized by the presence of a low-resistivity layer

FIG. 9. Curves of VES 8, VES 3, and VES 9 obtained over the center of the geothermal field. Numbers in bars designate interpreted true resistivities, in ohm-meters.

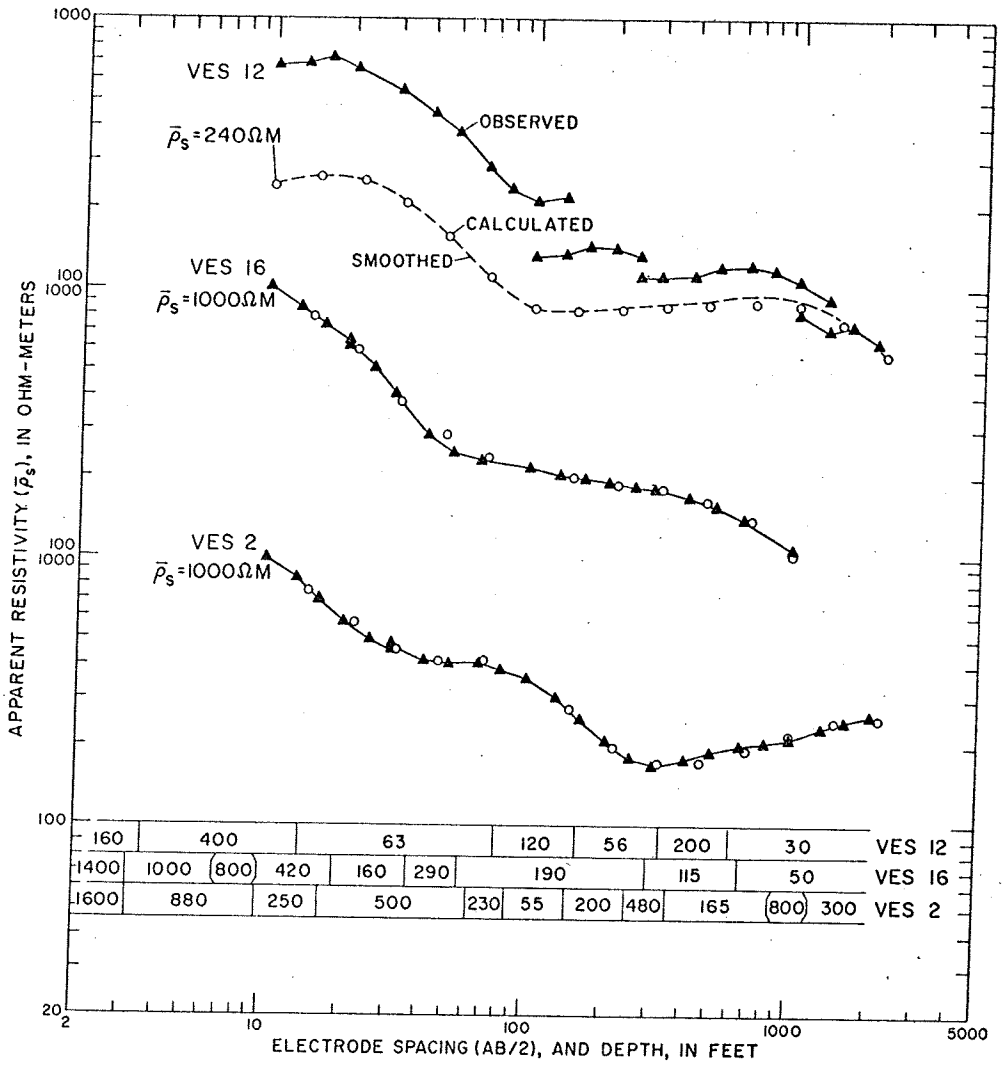

FIG. 11. Curves of VES 2, VES 12, and VES 16 obtained south of the southeastern boundary of the geothermal field. Numbers in bars designate interpreted true resistivities, in ohm-meters. Layering is based on automatically calculated models.

(2–6.5 ohm-m) above it, and a moderately resistive layer (~30 ohm-m) around it. It is interesting to note the similarity between this interpreted geoelectric section and the general model of a vapor-dominated system presented by White et al (1971). A simplified version of White's model is presented in Figure 12.

RESISTIVITY, SP, AND IP HORIZONTAL PROFILES

In 1971, two years after the VES data were obtained, horizontal profiles of resistivity, SP, and IP were made along the road from point *A* to *A'* (see Figure 1). The resistivity and the IP were measured at two electrode spacings of a three-electrode (AMN) array. The electrode spacings (AO) between the current electrode (A) and the center (O) of the potential electrodes (M and N) was 600 ft for one profile and 1000 ft for the other. The distance (MN) between the potential electrodes for both profiles was 400 ft. The SP measurements were made prior to the 600-ft resistivity measurement. The IP measurements were made

in the frequency domain at 0.1
the percent frequency effect (F
calculated using the formula

$$\mathrm{PFE} = \frac{(\bar{\rho}_{0.1} - \bar{\rho}_1}{\sqrt{\bar{\rho}_{0.1} \cdot \rho_1}}$$

where $\bar{\rho}_{0.1}$ and $\bar{\rho}_{1.0}$ are the app
measured at 0.1 and 1.0 hz, res

The lowest apparent resistiv
zontal profiling data were meas
ter of the geothermal field, whe
the 2- to 6.5-ohm-m layer is la
segment of the profiling data.
sistivity values measured with
1000 ft are larger than those m
smaller AO spacing of 600 ft. T
parent resistivity at larger elec
roborates the VES data interpr
the presence of a deep hig
(vapor-dominated layer) benea
resistivity cover. To the nort
thermal field, the apparent resis
low because of the presence o
lacustrine deposits in Hayde
southeast of the geothermal fi

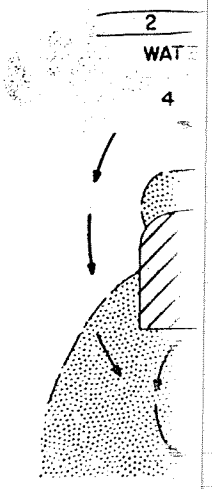

FIG. 12. Model of a vapor-domi
rich in sulfates. (2) Zone betwee
from condensing steam, is domina
conductive heat flow exists, with
section). (5) Vapor-dominated re
heat flow above which is a boilin

in the frequency domain at 0.1 and 1.0 hz, and the percent frequency effect (PFE) values were calculated using the formula

$$\mathrm{PFE} = \frac{(\tilde{\rho}_{0.1} - \tilde{\rho}_{1.0})}{\sqrt{\tilde{\rho}_{0.1} \cdot \rho_{1.0}}} \cdot 100,$$

where $\tilde{\rho}_{0.1}$ and $\tilde{\rho}_{1.0}$ are the apparent resistivities measured at 0.1 and 1.0 hz, respectively.

The lowest apparent resistivities of the horizontal profiling data were measured over the center of the geothermal field, where the thickness of the 2- to 6.5-ohm-m layer is largest. Along this segment of the profiling data, the apparent resistivity values measured with the AO spacing of 1000 ft are larger than those measured with the smaller AO spacing of 600 ft. This increase in apparent resistivity at larger electrode spacings corroborates the VES data interpretation in terms of the presence of a deep high-resistivity layer (vapor-dominated layer) beneath a shallower low-resistivity cover. To the northwest of the geothermal field, the apparent resistivity is generally low because of the presence of a thick section of lacustrine deposits in Hayden Valley. To the southeast of the geothermal field, a marked increase in apparent resistivity is observed on the resistivity profiles and a broad resistivity high is formed which extends to the southeastern boundary of the section. Within this broad resistivity high, there are three zones of lower resistivity which can be interpreted as due to alteration zones resulting from the upward movement of thermal waters at a time when near-surface geothermal activity may have existed to the southeast of the presently active zone.

SP measurements, referenced to the first station on the northwest end of the traverse, produced the broad, positive anomaly shown in Figure 13. The amplitude of the anomaly is small and may be attributed to a variety of electric potential producing effects. However, an experiment by Poldini (1938 and 1939) proved that upward-migrating water, confined within a column, produced a positive potential when a measurement was made near the top of the column with respect to an arbitrary distant point. The potential attributed to solutions moving through porous media has been observed by several investigators and is known by various names such as electrofiltration, streaming, flow, and electrokinetic potentials (Sato and Mooney, 1960). This type of

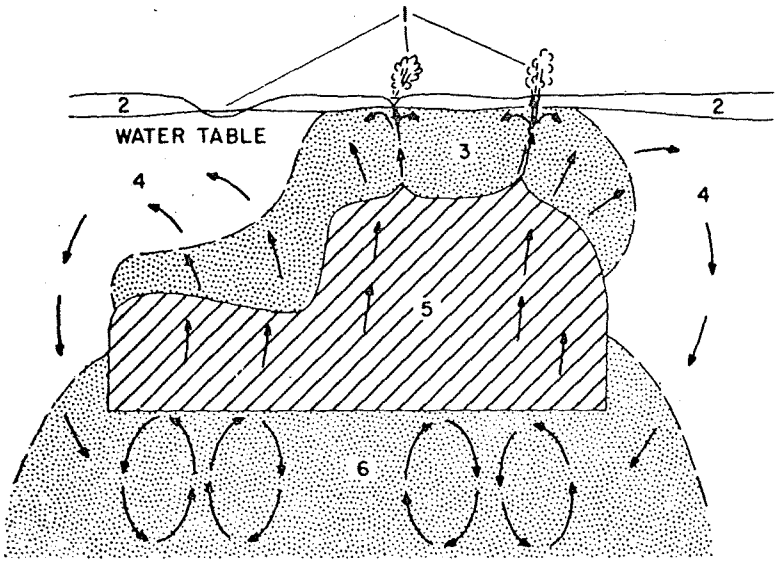

FIG. 12. Model of a vapor-dominated reservoir surrounded by water-saturated ground: (1) Springs and fumaroles rich in sulfates. (2) Zone between ground surface and water table. (3) Zone where liquid water, largely derived from condensing steam, is dominant (2–6.5-ohm-m layer in geoelectric section). (4) Zone where convective and/or conductive heat flow exists, with heat supplied from condensing steam in zone 3 (30-ohm-m layer in geoelectric section). (5) Vapor-dominated reservoir (75–130-ohm-m layer in geoelectric section). (6) Deep zone of convective heat flow above which is a boiling-water table (simplified from White et al, 1971).

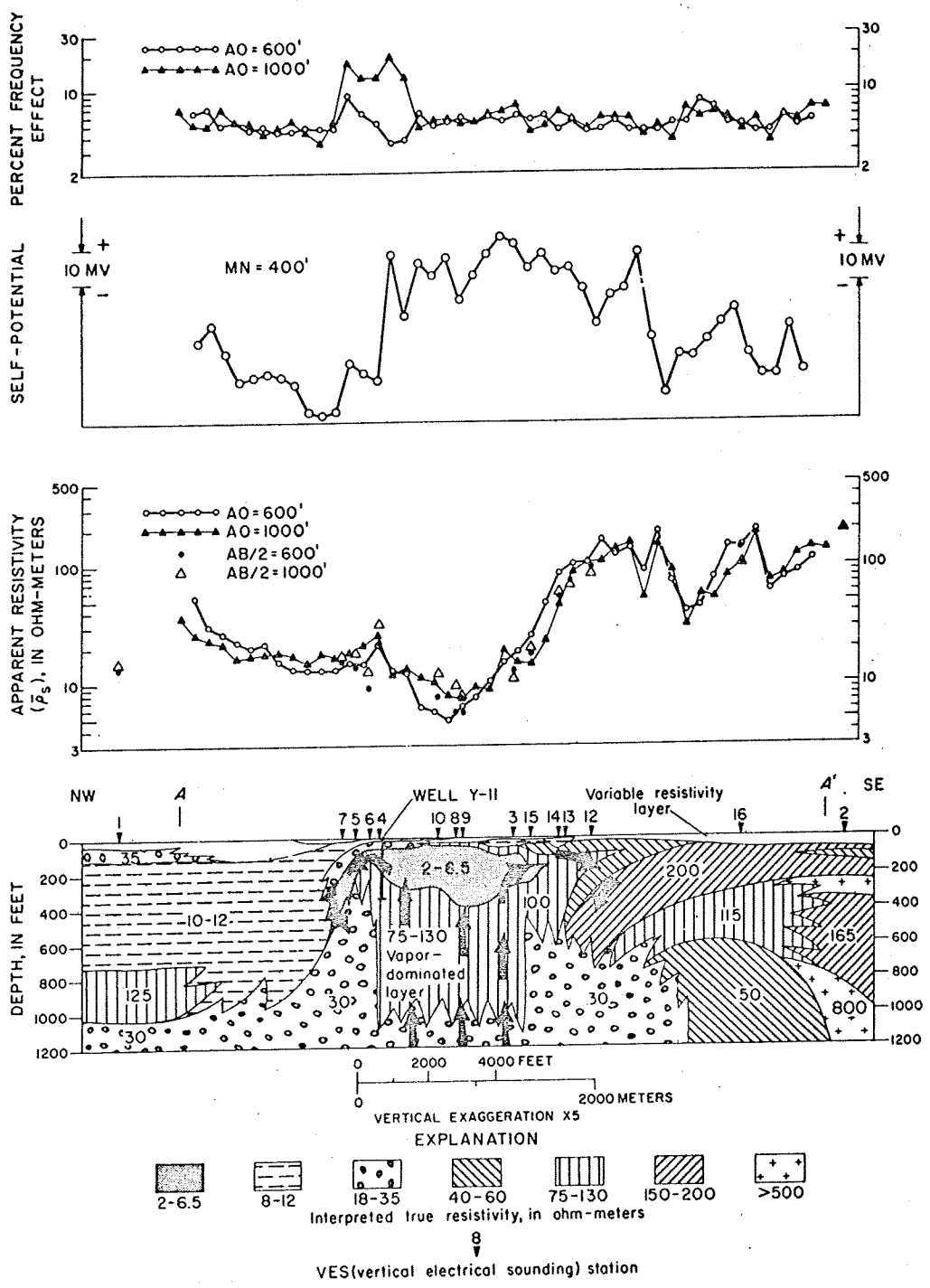

FIG. 13. Horizontal profiling data obtained with resistivity, SP, and IP (percent frequency effect). Arrows designate movement of steam and water. AO, distance from current electrode, A, to center of potential electrodes, O. MN, distance between potential electrodes. AB/2, Schlumberger-electrode spacing of VES curves.

potential is caused by cation
pore waters owing to the pr
of anions by the rock. The up
concentrate the cations near
in a positive anomaly over t
water.

On the basis of Poldini's w
to assume that the broad SP a
portion directly over the t
from upward-moving waters
vection currents emanating
ergy source. The low SP v
northwest edge of the therm
result of downward-moving
cycling process involved in
thermal waters (compare F
White et al, 1971).

The reason for the con
anomaly beyond the southe
geothermal field (as interpre
is not understood. Possibly,
amounts of the thermal wate
the ground surface move lat
they reach the more perme
low apparent resistivity do t
The downward-moving wate
observed low level of SP
zones of low resistivity.

The two IP profiles were
arithmic scale in the upper
The profiles are similar, bo
tively high IP ba kground
cent which is attri table to
of clayey materials and pyri
layers. Differences between
the amplitude of the obser
ticularly in the vicinity of the
of the inferred vapor-domi
crease in the polarization effe
by an increased quantity o
deposited by circulating the
the mineralogical analysis o
that pyrite exists from a de
the bottom of the well at 34
AO = 1000 ft anomaly is sig
that seen on the shorter sp
that the pyrite and its distri
depth at the boundary of t
sibly a similar pyrite enric
the small IP anomaly show
the vicinity of VES 16.

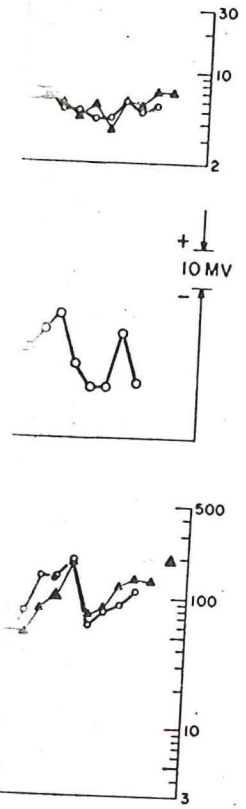

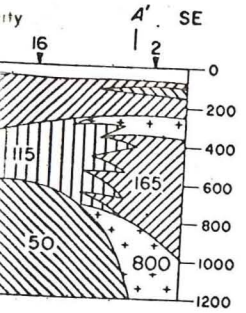

>500

ency effect). Arrows desig-
of potential electrodes, O.
ES curves.

potential is caused by cation enrichment of the pore waters owing to the preferential adsorption of anions by the rock. The upward-moving waters concentrate the cations near the surface resulting in a positive anomaly over the zone of migrating water.

On the basis of Poldini's work, it is reasonable to assume that the broad SP anomaly, at least the portion directly over the thermal zone, arises from upward-moving waters set in motion by convection currents emanating from the thermal energy source. The low SP values bordering the northwest edge of the thermal area are possibly a result of downward-moving waters, part of the cycling process involved in the movement of thermal waters (compare Figures 12 and 7 of White et al, 1971).

The reason for the continuation of the SP anomaly beyond the southeast boundary of the geothermal field (as interpreted from VES data) is not understood. Possibly, however, significant amounts of the thermal waters upon approaching the ground surface move laterally, and not until they reach the more permeable altered zones of low apparent resistivity do they begin to descend. The downward-moving water would produce the observed low level of SP coincident with the zones of low resistivity.

The two IP profiles were plotted on semilogarithmic scale in the upper part of Figure 13. The profiles are similar, both indicating a relatively high IP background level of about 5 percent which is attributable to a wide distribution of clayey materials and pyrite in the near-surface layers. Differences between the profiles occur in the amplitude of the observed anomalies, particularly in the vicinity of the northwest boundary of the inferred vapor-dominated zone. The increase in the polarization effect is probably caused by an increased quantity of disseminated pyrite deposited by circulating thermal waters. Indeed, the mineralogical analysis of well Y-11 indicates that pyrite exists from a depth of about 50 ft to the bottom of the well at 347 ft. The fact that the AO=1000 ft anomaly is significantly larger than that seen on the shorter spaced profile suggests that the pyrite and its distribution increases with depth at the boundary of the thermal zone. Possibly a similar pyrite enrichment exists beneath the small IP anomaly shown on both profiles in the vicinity of VES 16.

SUMMARY AND CONCLUSIONS

Vertical electrical soundings in the Mud Volcano area of Yellowstone National Park indicate that the vapor-dominated reservoir is characterized by high resistivities and that it occurs under a cover of very low resistivity. Because of this low-resistivity layer, reconnaissance surveys with horizontal profiling will delineate the thermally active zone by a low-resistivity anomaly. The boundaries of the geothermal field as defined by the quantitative interpretation of the VES curve is in excellent agreement with the approximate boundaries inferred from mapping the surface geology. Beneath VES 1 and VES 16, the geothermal conditions may exist at depths slightly greater than about 1000 ft, whereas beneath VES 2 the thermal activity, if it exists, must be at depths greater than 1500 ft.

The SP anomalies seem to be directly related and interpretable in terms of the thermal water circulation system, and although the SP anomaly observed in the Mud Volcano area is relatively small, its existence warrants the further study and measurement of SP in other geothermal areas.

The IP anomalies observed at the northwestern boundary and south of the southeastern boundary were interpreted in terms of pyrite concentrations deposited by sulfur-rich thermal waters at those locations where the thermal waters intermix with meteoric waters and begin a downward movement in the hydrological recycling process surrounding the geothermal cell.

REFERENCES

Alfano, L., 1961, Geolectrical explorations for natural steam near "Monte Amiata": Quad. Geofisica Appl., v. 21, p. 3–17.

Banwell, C. J., and MacDonald, W. J. P., 1965, Resistivity surveying in New Zealand thermal areas: Presented at 8th Commonwealth Mining and Metall. Cong., Australia and New Zealand, Paper 213, p. 1–7.

Breusse, J. J., and Mathiez, J. P., 1956, Application of electrical prospecting methods to tectonics in the search for natural steam at Larderello, Italy, *in* Geophysical case histories: Vol. II, Paul L. Lyons, Editor, Tulsa, SEG, p. 623–630.

Cheng, W. T., 1970, Geophysical exploration in the Tatun volcanic region, Taiwan: Geothermics Spec. Issue 2, v. 2, pt. 1, p. 262–274.

Deppermann, K., 1954, Die Abhängigkeit des scheinbaren Widerstandes vom Sondenabstand bei der Vierpunkt-Methode: Netherlands, Geophys. Prosp., v. 2, p. 262–273.

Duprat, A., 1970, Contribution of geophysics to the study of the geothermal region of Denizli-Saraykoy, Turkey: Geothermics Spec. Iss. 2, v. 2, pt. 1, p. 275–286.

Hatherton, T., MacDonald, W. J. P., and Thompson,

G. E. K., 1966, Geophysical methods in geothermal prospecting in New Zealand: Bull. Volcanol., v. 29, p. 485–498.
McEuen, R. B., 1970, Delineation of geothermal deposits by means of long-spacing resistivity and airborne magnetics: Geothermics Spec. Iss. 2, v. 2, pt. 1, p. 295–302.
Meidav, T., 1970, Application of electrical resistivity and gravimetry in deep geothermal exploration: Geothermics Spec. Iss. 2, v. 2, pt. 1, p. 303–310.
Orellana, Ernesto, and Mooney, H. M., 1966, Master tables and curves for vertical electrical sounding over layered structures: Madrid, Interciencia.
Poldini, E., 1938, Geophysical exploration by spontaneous polarization methods: Mining Mag., London, v. 59, p. 278–282, 347–352.
——— 1939, Geophysical exploration by spontaneous polarization methods: Mining Mag. London, v. 60, p. 22–27, 90–94.
Rijkwaterstaat, 1969, Standard graphs for resistivity prospecting: EAEG, Netherlands.
Risk, G. F., MacDonald, W. J. P., and Dawson, G. B., 1970, D.C. resistivity surveys of the Broadlands geothermal region, New Zealand: Geothermics Spec. Iss. 2, v. 2, pt. 1, p. 287–294.
Sato, Motoaki, and Mooney, H. M., 1960, The electrochemical mechanism of sulfide self-potentials: Geophysics, v. 25, p. 226–249.
White, D. E., Muffler, L. J. P., and Truesdell, A. H., 1971, Vapor-dominated hydrothermal systems compared with hot-water systems: Econ. Geol., v. 66, p. 75–97.
Zohdy, A. A. R., 1965, The auxiliary point method of electrical sounding interpretation and its relationship to the Dar Zarrouk parameters: Geophysics, v. 30, p. 644–660.
——— 1969, The use of Schlumberger and equatorial soundings in groundwater investigations near El Paso, Texas: Geophysics, v. 34, p. 713–728.
——— 1972, Automatic interpretation of resistivity sounding curves using modified Dar Zarrouk functions [abs.]: Geophysics, v. 38, p. 196–197.

QUANTITATIVE INT

G. J. PALACKY* AND

Recent improvements of t electromagnetic system hav more quantitative approac The necessary interpretatio tained in two ways: either b tem and ground EM measur ing computational or analog Both approaches have be former, the system decay ra with the apparent conduc

INTRODUCT

INPUT[1] (hereinafter refe system) is a towed-bird, tim tem whose first version was Barringer in the late 1950's most widely used AEM sys surveys were flown in 197 plained in Figure 1.

Brief description of the syste

The primary magnetic fie rent pulses which are 1.1 m in polarity. The emf due t netic field is measured at 0.48, 0.75, 1.10, 1.57, and transmitter switch-off. The over a time interval whi 0.22 msec to 0.54 msec.

The presence of a conduc erates in the receiver an superimposed upon the pr torts it, but subsequently as a decaying signal follow primary pulse.

[1] Registered Trademark of

† Manuscript received by the

* Now with Barringer Resear Ontario, Canada, M5S 1A7.
‡ University of Toronto, Toro